

Predicting planar motion behavior under contact uncertainty

JAN ROSELL *, LUIS BASAÑEZ and RAÚL SUÁREZ

Institute of Industrial and Control Engineering, Technical University of Catalonia, Barcelona, Spain

Received 30 July 2004; revised 16 November 2004; accepted 27 December 2004

Abstract—Performing complex assembly tasks with robots requires fine-motion planners able to cope with uncertainty and contact motions, and this is a recognized difficult issue. This paper proposes a method to predict the behavior of motions under contact uncertainty in order to check the feasibility of paths generated by gross-motion planning algorithms from a nominal model of the environment. This pragmatical approach enables the extension of gross-motion planning techniques to constrained-motion planning problems, ensuring the feasibility of the task despite the uncertainties. The approach has been implemented for assembly tasks in the plane with three degrees of freedom.

Keywords: Compliant motion; uncertainty; contact analysis; configuration space; robotic assembly.

1. INTRODUCTION

1.1. Problem statement

The execution of complex assembly tasks with robots may fail if it relies on trajectories obtained from the nominal description of the environment, since the uncertainty may not be small enough relative to the task clearance. Nevertheless, constrained motion planning (i.e., the planning of trajectories that explicitly take into account the effect of uncertainties and that make use of compliant motions based on sensory information of configuration and force) is a difficult issue and, in spite of the research effort done, not many practical results have been yet obtained. On the other hand, the field of gross-motion planning (i.e., the planning of robot trajectories without considering uncertainties) has given good results already transferred to industrial applications. Due to these facts, it seems an appealing issue to be able to check if, using a compliant control, a nominal free path (generated by a gross-motion planning algorithm) is feasible, i.e., if it allows to reach the goal despite possible contacts occurring during task execution due to uncertainty.

*To whom correspondence should be addressed. E-mail: jan.rosell@upc.es

1.2. Previous work

Most of the approaches to constrained motion planning follow fine-motion planning strategies. These strategies describe geometric trajectories as a function of the current actual situation during the task execution, assuming predefined compliant matrices. They can be gathered in three groups: (a) the LMT approach [1] that describes the synthesis of compliant motions as the backchaining of preimages from the goal region to the initial region, the preimage for a given velocity command being the set of configurations that guarantee that the goal is reachable and recognizable taking into account uncertainty in sensing and control [2, 3], (b) the two-phase planners which first generate a nominal plan assuming no uncertainty, and then consider uncertainty to replan the steps of the path that are error-prone [4–6] and (c) the contact-space approaches which represent the task as a graph of contact states and synthesize a plan by searching in this graph, considering the uncertainty in the states definition and in the state transition operators [7–10].

Other approaches to constrained motion planning assume a predefined trajectory and determine, either by learning [11, 12] or by analytical methods [13, 14], the error-corrective compliant matrix that allows the successful execution of the assembly task.

Despite the research done, the problem is still unsolved for 6-d.o.f. tasks and it is even not completely solved in a general way for planar assembly tasks. Previous referenced works present, from different perspectives, how to cope with uncertainty in robotized tasks requiring constrained motion planning. However, no systematic approach has been made covering and thoroughly considering all the uncertainty sources that may interfere in the task performance. The proposed approach is an attempt in this direction by predicting the motion behavior under all kinds of uncertainty sources in order to analyze the feasibility of the task execution.

1.3. Paper scope

This paper is focused on the prediction of the motion behavior when a nominal free path is followed in the execution of a 3-d.o.f. planar assembly task between polygonal objects and contact situations are possible due to uncertainty. We assume the existence of a compliant robot control. The proposed method can be considered as the second phase of a two-phase fine-motion planner.

Section 2 presents a basic background related to uncertainty, configuration space and reaction force analysis. Section 3 gives an overview of the proposed solution, which is developed in Section 4 and experimentally validated in Section 5. Finally, Section 6 discusses the proposed approach and its main contributions.

2. BACKGROUND

2.1. Uncertainty

Uncertainty sources can be classified as global or local, depending on their effects. A source of uncertainty is considered global if it determines the deviation of either all the topological elements of the manipulated object or of all the topological elements of all the static objects, otherwise it is considered local. Local sources of uncertainty can give rise to contact situations that are not possible for the nominal geometry and nominal position of the objects. The maximum deviations produced by the global and the local sources of uncertainty will be called ϵ_G and ϵ_L , respectively.

The following sources of uncertainty affect the performance of a robotized assembly task:

- (a) Manufacturing tolerances in the object shape and size. This is a local source since the deviation produced at each topological element is independent from the others (although this deviation imposes some constraints for neighboring topological elements).
- (b) Imprecision in the pose (position and orientation) of the static objects. The deviation in the pose of a static object determines the corresponding deviation in all its topological elements but it does not affect other possible static objects. Therefore, if there is only one static object, this source is global, and it is local if there is more than one.
- (c) Imprecision in the pose of the robot gripper. This is a global source since a deviation in the pose of the robot determines the corresponding deviations of all the topological elements of the manipulated object.
- (d) Imprecision in the pose of the object in the robot gripper. This is a global source for the same reason stated in source c.

2.2. Configuration space

Let \mathcal{A} and \mathcal{B} be two polygons describing, respectively, a manipulated object and a static object. Let $\{T\}$ and $\{W\}$ be the reference frames attached to the manipulated object \mathcal{A} and to the workspace, respectively. $\{T\}$ has the origin at the manipulated object reference point $O_{\mathcal{A}}$, and an orientation ϕ with respect to $\{W\}$.

Then, the configuration space (\mathcal{C} -space) of the manipulated object is the set of all its configurations, a configuration being specified by the position and orientation of $\{T\}$ with respect to $\{W\}$ [15].

For movements in the plane with three degrees of freedom the \mathcal{C} -space is $\mathbf{R}^2 \times S_{\rho}^1$, where S_{ρ}^1 is the circle of radius ρ , the gyration radius of the manipulated object. Then, a configuration is described by three generalized coordinates (x, y, q) , with $q = \rho\phi$, all having units of length. Vector orthogonality in \mathcal{C} -space makes physical sense in terms of energy if ρ is the gyration radius of the manipulated object [16]. The x and y coordinates of the \mathcal{C} -space represent the position of $O_{\mathcal{A}}$ with respect to

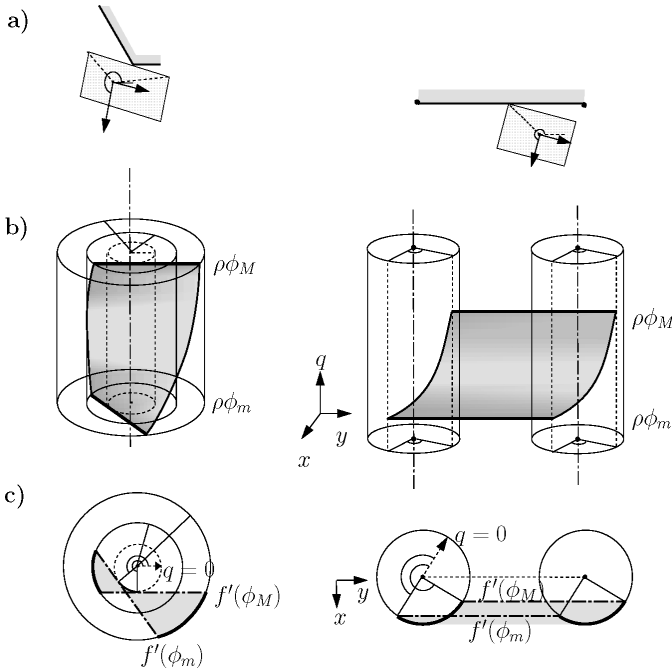


Figure 1. Type-A and a type-B basic contacts in (a) physical space; (b) \mathcal{C} -space and (c) \mathcal{C}' -space.

$\{W\}$; therefore, the \mathcal{C} -space reference frame has the x -axis and the y -axis coincident with those of $\{W\}$. The set of configurations that do not produce interference between objects is denoted $\mathcal{C}_{\text{free}}$.

The parameterized translational configuration space (\mathcal{C}' -space) is defined as the set of projections onto the xy -plane ($q = 0$) of the \mathcal{C} -space slices for all the possible orientations of the manipulated object, using the orientation as a parameter [17]. Contact constraints are easily determined using this representation, which is also useful for the uncertainty analysis.

As an example Fig. 1a shows, in the physical space, a contact between an edge of \mathcal{A} and a vertex of \mathcal{B} (type-A basic contact), and a contact between a vertex of \mathcal{A} and an edge of \mathcal{B} (type-B basic contact). Figure 1b shows, in the \mathcal{C} -space, the corresponding set of configurations where these contacts takes place (\mathcal{C} -faces) and Fig. 1c their representation in \mathcal{C}' -space. The \mathcal{C} -faces are ruled surfaces with ruling segments parallel to the plane $q = 0$ and ranging from the minimum (ϕ_m) to the maximum (ϕ_M) orientations where the contact can take place. The ruling segments are represented as f' in \mathcal{C}' -space [17].

2.3. Reaction force analysis

Consider a basic contact at a contact configuration c_o , and let (Fig. 2) [16]:

- \vec{n} be the unitary vector normal to the \mathcal{C} -face at c_o .

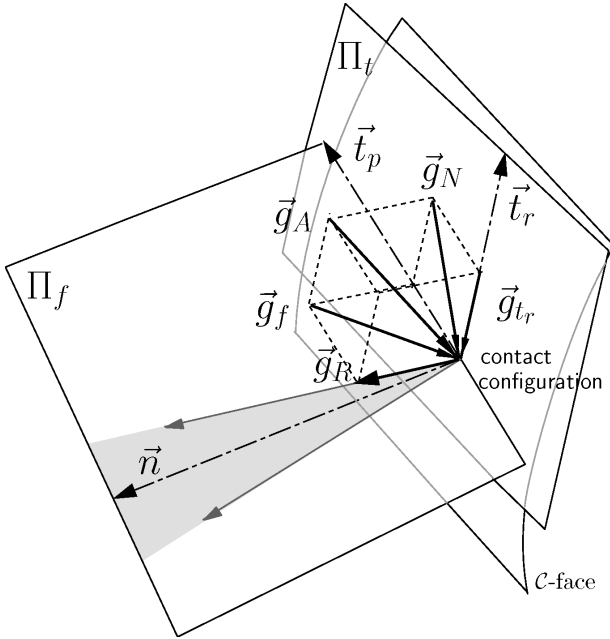


Figure 2. Force decomposition in \mathcal{C} -space.

- \vec{t}_r be the unitary vector in the direction of pure rotation around the physical contact point. Positive motions along \vec{t}_r correspond to rotations that increase ϕ .
- \vec{t}_p be the unitary vector in the direction orthogonal to \vec{t}_r and \vec{n} . The sense of \vec{t}_p makes $[\vec{t}_r, \vec{t}_p, \vec{n}]$ right-handed.
- The generalized friction cone be the set of all possible generalized reaction forces arising at c_0 .
- Π_t be the plane tangent to the \mathcal{C} -face at c_0 .
- Π_f be the friction plane. Π_f contains the generalized friction cone and is orthogonal to \vec{t}_r at c_0 .

Vectors $[\vec{t}_r, \vec{t}_p, \vec{n}]$ form an orthogonal reference frame, known as contact reference frame, with origin at the contact configuration. The contact reference frame is used to analyze the effect of a force applied at the contact configuration. An applied generalized force \vec{g}_A that points into a \mathcal{C} -face is decomposed into \vec{g}_f and \vec{g}_{t_r} , \vec{g}_f being the projection on the plane Π_f and \vec{g}_{t_r} the component along \vec{t}_r . Then, the reaction force \vec{g}_R is $\vec{g}_R = -\vec{g}_f$ if \vec{g}_f is inside the generalized friction cone; otherwise \vec{g}_R is the projection of $(-\vec{g}_f)$ along the direction of \vec{t}_p onto the edge of the friction cone. Finally, the net force \vec{g}_N that defines the direction of motion is the projection of \vec{g}_A , along the direction of \vec{g}_R , onto the plane Π_t (Fig. 2) [16].

This force analysis will be done using the dual representation of forces in order to take more easily into account the uncertainty. This representation maps the supporting line of a force into a point (that represents the force direction) and a

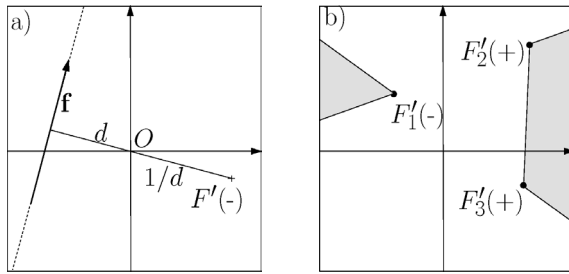


Figure 3. (a) A force \mathbf{f} and its dual representation F' . (b) Linear combination of three dual forces, one of them with a different sign from the others.

sign (that expresses the force sense), and is useful for the analysis of planar contact problems [18].

Using the dual representation, the reaction force $\mathbf{f} = (f_x, f_y)$ and torque τ with respect to a reference origin O , produced at a contact situation during a planar assembly task, are mapped into the point $F' = (f_y/|\tau|, -f_x/|\tau|)$ plus the sign of τ . Geometrically, F' lies on the normal to the force line through the reference origin O and at a distance $1/d$ from O , d being the distance between the force line and O (Fig. 3a).

Some relevant properties of the dual representation of forces are:

1. The supporting line $ax + by + c = 0$ of a force \mathbf{f} maps into the point $F' = (a/c, b/c)$ (Fig. 3a).
2. The lines of forces passing through a point map into points of a line, called the dual line of the point.
3. The lines of forces lying inside a cone $\widehat{r_1 r_2}$ map into points inside a cone $\widehat{r'_1 r'_2}$ with vertex on the origin, r'_1 and r'_2 being orthogonal to r_1 and r_2 , respectively.
4. The lines of forces passing through a point P and lying inside a cone \widehat{ab} , map into points of a segment $\overline{A'B'}$, A' and B' being the dual points of lines a and b , respectively.
5. A force \mathbf{f} resulting of a non-negative linear combination of two forces \mathbf{f}_1 and \mathbf{f}_2 with dual representations F'_1 and F'_2 with the same sign maps into a point F' on the segment $\overline{F'_1 F'_2}$, plus the same sign as F'_1 and F'_2 ; if F'_1 and F'_2 have different signs, F' lies on one of the two portions of the straight line defined by F'_1 and F'_2 removing the segment $\overline{F'_1 F'_2}$, with the sign of F'_1 if F' lies on the portion bounded by F'_1 or the sign of F'_2 otherwise. This rule can recursively be applied to the nonnegative linear combination of several forces (Fig. 3b).

3. SOLUTION OVERVIEW

As it has been stated, the objective is to verify if, using a compliant control, a nominal free path (generated by a gross-motion planning algorithm) allows to reach

the task goal, despite possible contacts occurring during task execution. With this aim, the following solution is proposed.

A nominal free path is adequate to perform an assembly task subject to uncertainty if one of the following conditions holds:

- Contacts are not possible along the path.
- Contacts might occur but either the robot can comply at them and proceed towards the goal or, if this is not the case, the contact situation can be identified with certainty and a recovery path can be planned and executed.

In the proposed solution, these conditions are tested at a finite set of configurations of the nominal free path. Depending on the effect of the uncertainty, a given configuration can be [19]:

- **Compatible:** a configuration c is called compatible if, taking into account uncertainty, a contact situation can take place at c .
- **Motion-feasible:** a compatible configuration c is called motion-feasible for a given commanded velocity \mathbf{v} if \mathbf{v} produces the same kind of motion (same sense of rotation and displacement) at all the basic contacts that can take place at c , and the resulting motion is error-corrective.
- **Distinguishable:** a compatible configuration c is called distinguishable if all of the contact situations that can take place at c can be unambiguously identified.

Then, a configuration of a path is classified as:

- **Free:** if it is not compatible.
- **Compliant:** if it is compatible and motion-feasible.
- **Guarded:** if it is compatible and distinguishable but not motion-feasible.
- **Ambiguous:** if it is compatible and neither distinguishable nor motion-feasible.

Finally, a path is classified as:

- **Free:** if it contains only free configurations.
- **Compliant:** if it does not contain any guarded nor ambiguous configurations and it contains at least one compliant configuration.
- **Guarded:** if it does not contain any ambiguous configurations and at least it contains one guarded configuration.
- **Ambiguous:** if it contains at least one ambiguous configuration.

The path is feasible if it is either free, compliant or guarded. If the path is free it can be followed as a gross-motion path. If the path is compliant it can be followed complying at contacts when they occur. In both cases the path can be followed with the guarantee that the task will be successfully completed. If the path is guarded a recovery motion must be planned to move away from the non motion-feasible contact situation (which is known with certainty). Finally, if the path is ambiguous it is not feasible, since it cannot be followed with the guarantee that the task will be successfully completed and from any ambiguous configuration it is not possible to plan sure recovery strategies.

Therefore, in order to determine the path feasibility three basic problems have to be tackled:

- Given a configuration of the path, determine if it can become a contact configuration due to uncertainties. For this purpose, the set of contact situations that can take place at the given configuration must be computed. This is done using the Compatibility Tool (Section 4.1).
 - Given a compatible configuration, determine the direction of the possible contact motion when the nominal command is applied. This is done using the Motion Analysis Tool (Section 4.2).
 - Given a compatible and non motion-feasible configuration, determine if the possible contact situations can be unambiguously identified using force information when contact occurs. This is done using the Distinguishability Tool (Section 4.3).
- These tools are combined in the Path-Evaluation algorithm (Section 4.4).

4. THEORETICAL DEVELOPMENTS AND RESULTS

4.1. Compatibility tool

4.1.1. Overview. Contact situations have been described in the literature basically in terms of topological elements, or in terms of forces/torques, depending on the needs and convenience of each approach [10]. In the approach proposed here, the analysis of a set of configurations of a given precomputed geometric path has to be done and, since the occurrence of a contact situation at a given configuration only depends on the task geometry and uncertainty, then the most natural way to perform the compatibility analysis is to use the nominal \mathcal{C}' -space and the Configuration Domains that capture the effect of uncertainty. Given a configuration c , to test if it is compatible with a contact situation, a Configuration Domain is constructed and positioned with respect to c . Then, in the presence of uncertainty, c may become a contact configuration if the Configuration Domain intersects the nominal \mathcal{C}' -space corresponding to that contact situation. In the following subsections the effect of uncertainty is analyzed and captured into the Configuration Domains. Finally, the procedure to test the compatibility is presented.

4.1.2. Analysis of the effect of uncertainty. Consider a basic contact and let ϵ_v and ϵ_{t_v} be the maximum deviation in the position of the contact vertex due to the imprecision in the positioning of the objects and the manufacturing tolerances, respectively. Let also ϵ_e and ϵ_{t_e} be defined in an equivalent way for the ends of the contact edge.

Let e be the actual contact edge and e_0 be its nominal model located at its nominal position. Due to uncertainty, e can be in different positions and orientations satisfying two conditions:

1. The vertices of e must lie inside the uncertainty circles of radius ϵ_e centered at the vertices of e_0 .

2. The length l of e must satisfy $l \in [l_0 - 2\epsilon_{te}, l_0 + 2\epsilon_{te}]$, l_0 being the length of e_0 .

Using these conditions, the set of possible realizations of e for a given deviation β in its orientation with respect to the orientation of e_0 is determined as follows. The region $\mathbf{R}_e(\beta)$ where vertex P of e lies is the intersection of the circle of radius ϵ_e centered at vertex P_0 of e_0 with the union of circles of the same radius centered at the end of e for all the possible realizations of e due to its variable length (Fig. 4a). The region $\mathbf{E}(\beta)$ that contains all the possible realizations of e for a deviation β is the positive linear combination of the regions $\mathbf{R}_e(\beta)$ of its two ends (Fig. 4b). $\mathbf{E}(\beta)$ can be partitioned into three disjoint parts, $\mathbf{L}_r(\beta)$, $\mathbf{L}_{P_a}(\beta)$ and $\mathbf{L}_{P_b}(\beta)$, as shown in Fig. 5a ($\mathbf{L}_r(\beta)$ is the rectangle of maximum area inscribed in $\mathbf{E}(\beta)$). Regions $\mathbf{L}_{P_a}(\beta)$ and $\mathbf{L}_{P_b}(\beta)$ are combined to form the geometric figure $\mathbf{L}(\beta)$, shown in Fig. 5b, that is used in the construction of the Configuration Domains.

Let Q be the contact vertex and e_m and e_M be its adjacent edges, such that e_M is first encountered when the border of the object is followed counterclockwise. Let also α_m and α_M be the deviations in the orientations of e_m and e_M , respectively. Then, the region $\mathbf{V}(\alpha_m, \alpha_M)$, where the contact vertex may lie is $\mathbf{V}(\alpha_m, \alpha_M) = \mathbf{R}_{e_m}(\alpha_m) \cap \mathbf{R}_{e_M}(\alpha_M)$. Nevertheless, in order to simplify the contact analysis, a more conservative but simpler region is next proposed.

Let $[\phi_m, \phi_M]$ be the range of orientations where a basic contact can occur for the nominal geometry, and let Δ_ϕ be the difference between an orientation ϕ and the nearest limit of the nominal range when $\phi \notin [\phi_m, \phi_M]$ and zero otherwise. Then, for a deviation $\alpha_M < 0$ in the orientation of e_M , the contact can occur at an orientation of the manipulated object $\phi > \phi_M$, for any possible value of α_m . The same happens exchanging M by m and the inequality signs. Therefore, in order to determine if a contact situation can occur at ϕ , region $\mathbf{V}(\alpha_m, \alpha_M)$ is simplified to region $\mathbf{V}(\alpha) \supseteq \mathbf{V}(\alpha_m, \alpha_M)$, defined as follows:

$$\mathbf{V}(\alpha) = \begin{cases} \mathbf{V}(\alpha, 0) = \mathbf{R}_{e_m}(\alpha) & \text{if } \phi \leq \phi_m \\ \mathbf{V}(0, 0) = \mathbf{C}(Q, \epsilon_v) & \text{if } \phi_m < \phi < \phi_M \\ \mathbf{V}(0, \alpha) = \mathbf{R}_{e_M}(\alpha) & \text{if } \phi \geq \phi_M, \end{cases} \quad (1)$$

$\mathbf{C}(Q, \epsilon_v)$ being a circle of radius ϵ_v centered at Q .

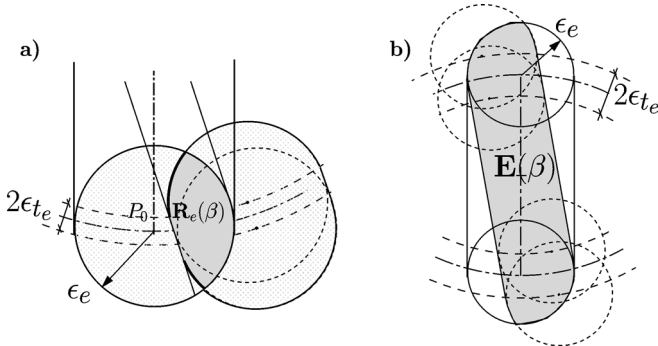


Figure 4. Uncertainty regions in physical space: (a) region $\mathbf{R}_e(\beta)$; (b) region $\mathbf{E}(\beta)$.

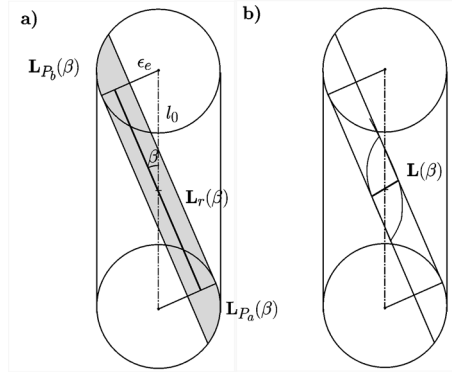


Figure 5. Representation in physical space of (a) partition of $\mathbf{E}(\beta)$ into three disjoint regions $L_r(\beta)$, $L_{P_a}(\beta)$ and $L_{P_b}(\beta)$; (b) geometric figure $L(\beta)$.

Finally, the sensing uncertainty is considered. The sensing uncertainty in the robot position affects the positions of all the geometrical elements of the grasped object. Then, for these elements, the effect of the sensing uncertainty in the robot position can be approximated by computing $\mathbf{E}(\beta)$ and $\mathbf{V}(\alpha)$ with the uncertainty radius enlarged by this sensing uncertainty. On the other hand, due to the sensing uncertainty, the actual robot orientation lies within a range around the measured one. Nevertheless, it can be proved that for the contact analysis it is only necessary to consider a single orientation ϕ_o of that range. ϕ_o is the orientation where the robot position is closest to the nominal contact positions. Then, the Configuration Domains described in the next section are, in fact, Position Domains defined for orientation ϕ_o .

4.1.3. Configuration Domains. Contact Position Domains allow easily handling of contact analysis because they capture the effect of uncertainty and permit to do the tests with the nominal \mathcal{C}' -space.

For a given basic contact i , the segment $f'_i(\phi)$ represents the nominal contact positions for the orientation ϕ . Then, if the contact can take place at a given configuration, its associated Contact Position Domain intersects $f'_i(\phi)$ for some orientation $\phi = \phi_o$.

For an orientation $\phi_o \in [\phi_m, \phi_M]$ the contact can take place for deviations $\alpha = \beta = 0$ (for which the areas of $V(\alpha)$ and $E(\beta)$ are maximum), whenever $V(0)$ and $E(0)$ overlap. Then, in this case, the Contact Position Domain is the circle centered at the position (x_o, y_o) corresponding to configuration c and obtained as the convolution of the circles $V(0)$ and $L(0)$. For an orientation $\phi_o \notin [\phi_m, \phi_M]$ the contact can take place only for deviations α and β satisfying $\beta - \alpha = \Delta_{\phi_o}^i$, whenever $V(\alpha)$ and $E(\beta)$ overlap. In this case the Contact Position Domain is constructed as follows.

For an orientation ϕ_o and a basic contact i , the Contact Position Set $\mathbf{u}^i(\alpha, \beta)$ is defined as the set of all the possible contact positions associated to (x_o, y_o) . If

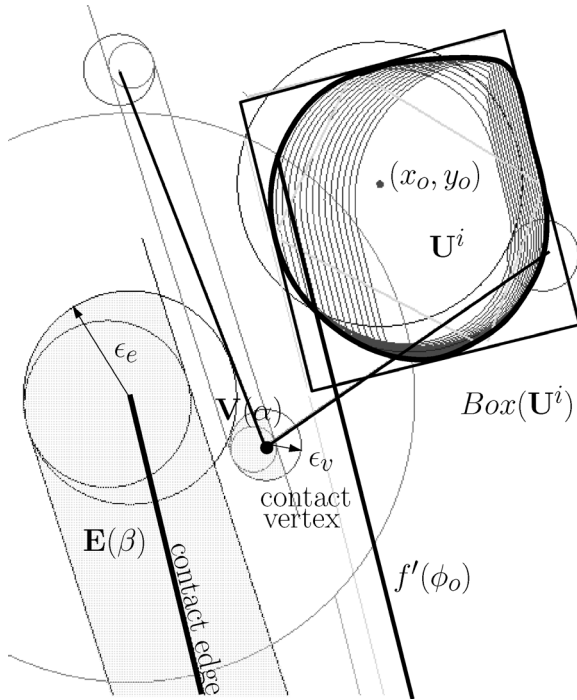


Figure 6. Contact position domain \mathbf{U}^i and its bounding box for an orientation $\phi_0 > \phi_M$.

$\mathbf{V}(\alpha)$ and $\mathbf{E}(\beta)$ overlap, i.e. the contact can take place, then $\mathbf{u}^i(\alpha, \beta)$ intersects the segment that represents the contact positions for the deviations α and β . The Contact Position Set is computed as the convolution of $\mathbf{V}(\alpha)$ with $\mathbf{L}(\beta)$, and centered at (x_0, y_0) , and its border is composed of five arcs of circumference and two straight segments.

The Contact Position Region $\mathbf{U}^i(\alpha, \beta)$ is defined as the region resulting of applying a transformation (rotation and translation) to $\mathbf{u}^i(\alpha, \beta)$ in such a way that when $\mathbf{V}(\alpha)$ and $\mathbf{E}(\beta)$ overlap, $\mathbf{U}^i(\alpha, \beta)$ intersects $f'_i(\phi_0)$.

Then, the Contact Position Domain \mathbf{U}^i is constructed as the union of a finite set of Contact Position Regions with values (α, β) satisfying $\beta - \alpha = \Delta^i_{\phi_0}$, but the border of \mathbf{U}^i is not analytically computed. Figure 6 shows the Contact Position Domain as the union of a finite set of 15 Contact Position Regions and its oriented bounding box, called $\text{Box}(\mathbf{U}^i)$.

For a contact situation involving a set S of basic contacts, the Contact Position Domain must simultaneously take into account the effect of the global sources of uncertainty and independently consider the local ones. Let \mathbf{U}^i_G and \mathbf{U}^i_L be the Contact Position Domains of contact $i \in S$ for the global and the local sources of uncertainty, respectively [20]. Let also \mathbf{U}^i_S be defined as $\mathbf{U}^i_S = \cap_{v_i \in S} \mathbf{U}^i_G$. Then, the Contact Position Domain \mathbf{U}^i of a contact $i \in S$ is equal to \mathbf{U}^i_L centered at the point $(x_i, y_i) \in \mathbf{U}^i_S$ closest to $f'_i(\phi_0) \forall i \in S$.

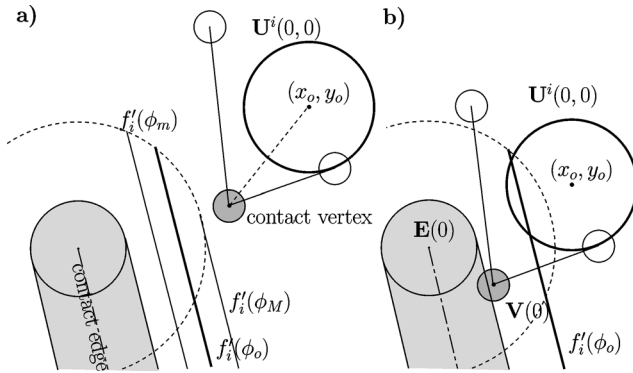


Figure 7. Compatibility of two configurations with a type-B basic contact in both physical space and C' -space: (a) non-compatible; (b) compatible.

If the nominal contact situation is possible at orientation ϕ_o , then U_L^i is a circle of radius ϵ_L and U_G^S is a circle of radius ϵ_G . Otherwise, U_L^i is computed following the procedure used for Contact Position Domains of a single contact and U_G^S is approximated by $U_G^S = \bigcap_{v_i \in S} \text{Box}(U_G^i)$.

4.1.4. Compatibility procedure. The compatibility procedure uses the nominal C' -space and the Contact Position Domains.

In the presence of uncertainty, a free configuration can be a contact configuration of a basic contact i if and only if the corresponding Contact Position Domain intersects the segment $f'_i(\phi_o)$ that represents the nominal contact positions for the test orientation ϕ_o . Since the Contact Position Domain is built as the union of Contact Position Regions this test is done by verifying if any of them intersects $f'_i(\phi_o)$.

In Figs 7 and 8 two examples are shown where compatibility with a type-B basic contact is illustrated in both the physical space and in the C' -space (darker lines). Figure 7 shows two configurations with the same orientation $\phi_o \in [\phi_m, \phi_M]$: Fig. 7a corresponds to a non-compatible configuration because $U^i \cap f'_i(\phi_o) = \emptyset$ due to the fact that $V(\alpha)$ and $E(\beta)$ do not overlap; Fig. 7b, in contrast, corresponds to a compatible configuration, since the opposite situation occurs. Figure 8 shows a configuration with an orientation $\phi_o > \phi_M$. The configuration is compatible because as shown in Fig. 8b $U^i(\alpha_2, \beta_2) \cap f'_i(\phi_o) \neq \emptyset$ due to the fact that $V(\alpha)$ and $E(\beta)$ do overlap, although this is not the case for the deviations of Fig. 8a.

For a contact situation involving a set S of basic contacts, U_G^S is computed for the set, and $U_L^i \forall i \in S$ are computed for each basic contact. Then, the contact analysis is independently done for each contact, and the multi-contact situation is possible if U_L^i intersects $f'_i(\phi_o) \forall i \in S$.

As an example, Fig. 9 shows a contact situation with two type-B basic contacts, #1 and #2, involving two different static objects. In this case, U_G^S , U_L^1 and U_L^2 are circles.

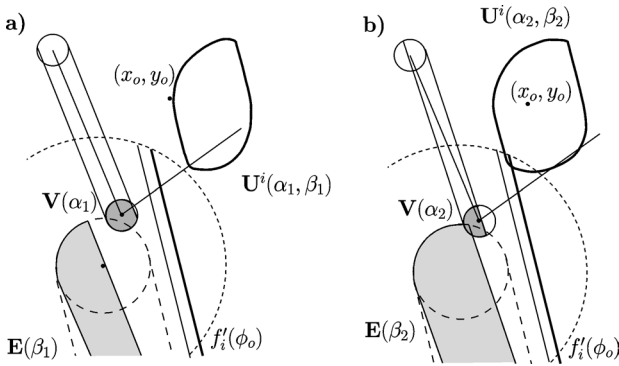


Figure 8. Compatibility analysis of a configuration (x_0, y_0, ϕ_0) with $\phi_0 > \phi_M$, illustrated in both physical space and C' -space for two values of (α, β) . (a) $V(\alpha_1)$ and $E(\beta_1)$ and, therefore, $U^i(\alpha_1, \beta_1)$ and $f'_i(\phi_0)$, do not overlap. (b) $V(\alpha_2)$ and $E(\beta_2)$ and, therefore, $U^i(\alpha_2, \beta_2)$ and $f'_i(\phi_0)$, do overlap, showing that the configuration is compatible.

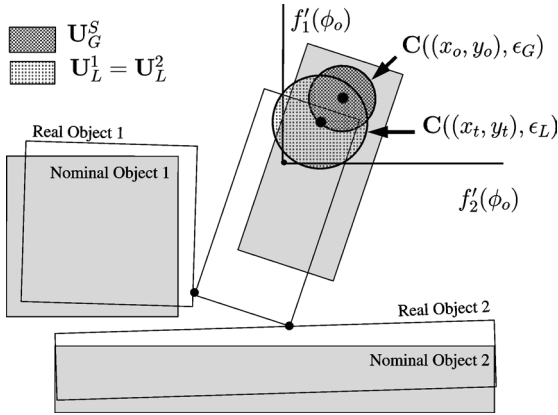


Figure 9. Compatibility determination with a contact situation involving two basic contacts.

The current configuration of the manipulated object may actually correspond to a contact configuration because U_L^1 intersects $f'_1(\phi_0)$ and U_L^2 intersects $f'_2(\phi_0)$.

4.2. Motion analysis tool

4.2.1. Overview. This tool performs the analysis of the motion at a given compatible configuration when the planned commanded velocity is applied. To do it, Motion Regions, representing the sets of commanded velocities that produce the same kind of motion of the manipulated object, are associated to each basic contact. Commanded velocities that produce either an uncertain motion, or a break of contact, or a sticking situation are not classified into any Motion Region. Then, the motion analysis tool verifies if a compatible configuration is motion-feasible by testing if the commanded velocity belongs to a Motion Region and if the resulting compliant motion is error-corrective. For a situation with multiple basic contacts

to be motion-feasible, the commanded velocity must be independently classified as motion-feasible for each basic contact and the Motion Region for each basic contact must be the same. In the following subsections Motion Regions considering the effect of uncertainty are described. Then, the procedure to test the motion feasibility is presented.

4.2.2. Motion Regions. A Motion Region associated to a basic contact is the set of commanded velocities that produce movements of the manipulated object in contact with the environment in a given sense of sliding and a given sense of rotation around the contact point. There are six Motion Regions:

$$\begin{array}{ll} \text{Region 1: } S^+ \wedge R^- & \text{Region 2: } S^+ \wedge R^+ \\ \text{Region 3: } S^- \wedge R^+ & \text{Region 4: } S^- \wedge R^- \\ \text{Region 5: } S^0 \wedge R^- & \text{Region 6: } S^0 \wedge R^+ \end{array}$$

where:

- R^+ and R^- represent the positive (or zero) and the negative rotation around the contact point, respectively.
- S^+ and S^- represent the positive and negative sliding of the contact point, respectively.
- S^0 , the border between S^+ and S^- , represents the no sliding motion due to the effect of friction.

These Motion Regions are computed in the dual force space, taking into account that this space is related with the generalized force space F_3 as follows: a plane $\Pi \subset F_3$ and its normal direction \mathbf{n} are represented in the dual force space by a line π' and a point N' , respectively, such that π' and N' maintain between them a relation of duality, i.e., N' can be obtained as the dual point of π' . Using this, the planes defined by the contact reference frame (Section 2.3) are mapped into lines that, together with the dual representation of the friction cone, partition the dual plane into Motion Regions. The algorithm given in Fig. 10 details the steps of this procedure, which is illustrated in Fig. 11a for a type-A basic contact.

When uncertainty is present, Motion Regions shrink because the lines and points defining the motion regions become themselves regions corresponding to applied forces that may produce different contact motions. Uncertainty is considered as shown in the following items and propagated through the steps of the procedure presented in Fig. 10 making use of the properties of the dual representation of forces:

- The uncertainty in the position of the contact point is considered by substituting the contact point by a segment centered at the contact point and parallel to the contact edge, such that all possible reaction forces cross this segment.
- The uncertainty in the orientation of the contact edge is considered by substituting the normal direction by a cone. The friction cone is enlarged accordingly.

Figure 11b shows the effect of uncertainty in the example presented in Fig. 11a (border regions are expressed as \mathcal{U} with a subindex indicating the original point or line).

- Dual-plane-partition**
- (1) Represent the vector \mathbf{t}_r by the point T'_r (which coincides with the contact point).
 - (2) Represent the vector \mathbf{n} by the dual point N' of the line normal to the contact edge passing through the contact point (T'_r).
 - (3) Represent Π_f by the dual line π'_f of the point T'_r .
 - (4) Represent Π_t by the dual line π'_t of N' .
 - (5) Represent the vector \mathbf{t}_p by the intersection point T'_p of lines π'_f and π'_t .
 - (6) Represent the friction cone as the dual segment FC of the physical friction cone.
 - (7) Label the negative and positive linear combination of T'_r and FC as regions 5 and 6, respectively.
 - (8) Label regions 1 to 4 (bounded by π'_f , π'_t and the border of regions 5 and 6), according to their characteristics.

Figure 10. Dual-space-partition algorithm.

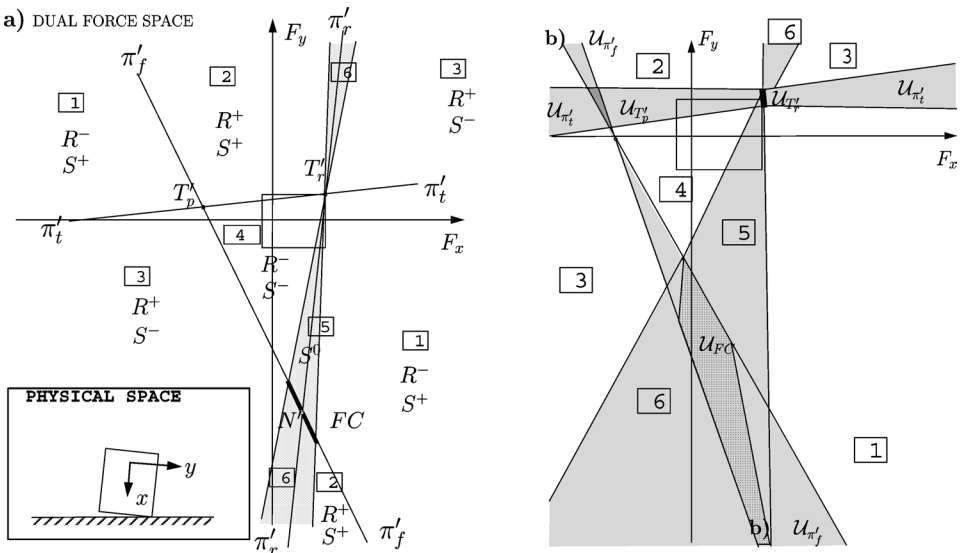


Figure 11. Dual space partition (a) without uncertainty, (b) with uncertainty.

4.2.3. Motion analysis procedure. The motion analysis procedure verifies the satisfaction of the following two conditions to label a configuration c as motion-feasible:

- The commanded velocity is classified into the same motion region for all the basic contacts that can take place at c in the presence of uncertainty. For each basic contact, the applied generalized force associated to the commanded velocity is classified into a motion region M if its dual representation, F' , satisfies $F' \in M$.
- The commanded velocity is error-corrective for all the basic contacts that can take place at c . For each basic contact the commanded velocity applied at c is error-corrective if the configuration c' , located at a distance $\epsilon_G + \epsilon_L$ from c along the path, is outside the \mathcal{C} -face of the basic contact.

4.3. The distinguishability tool

4.3.1. Overview. The knowledge of the contact force at a configuration where several contact situations can take place due to uncertainty can permit, in some cases, the identification of which one actually occurs. The distinguishability analysis determines, using force information, if this identification can be done. For each possible contact situation a generalized force domain is constructed containing all the possible reaction forces that can arise when that contact situation takes place. Then, contact situations are distinguishable if the corresponding generalized force domains do not intersect. In the following subsections the generalized force domains are first defined and constructed using the dual representation of forces. Then, the procedure to test the distinguishability is presented.

4.3.2. Generalized force domains. Let the generalized force domain \mathbf{G}_S associated to a configuration c compatible with a contact situation C_S , be the set of the generalized reaction forces that may arise when C_S takes place at c .

The generalized force domain \mathbf{G}_i of a contact situation with only one basic contact i is composed of the forces satisfying the following two conditions:

- Contact-point condition: the line of the reaction force must intersect the region $\mathbf{V}(\alpha)$ where the contact vertex lies. This region can be represented in a conservative way by a segment parallel to the contact edge \overline{MN} in Fig. 12), such that all the lines of forces intersecting $\mathbf{V}(\alpha)$ also intersect the segment.
- Direction condition: The reaction force direction must belong to the range $\psi \pm \Delta\psi$, where ψ is the orientation of the outward normal of the nominal contact edge e_0 and $\Delta\psi$ is computed considering the effect of friction and the maximum possible deviation in the orientation of the edge due to the uncertainty.

Let (Fig. 12):

- a and c be the straight lines with orientation $\psi - \Delta\psi$ passing through the extremes of \overline{MN} .
- b and d be the straight lines with orientation $\psi + \Delta\psi$ passing through the extremes of \overline{MN} .
- \mathbf{W} be the region where the lines of forces of \mathbf{G}_i lie; it is the union of cones \widehat{ab} and \widehat{cd} .

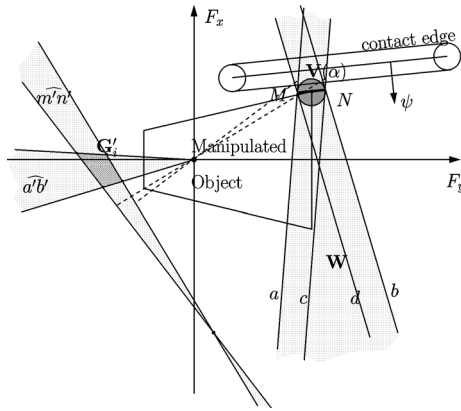


Figure 12. Dual representation of \mathbf{G}_i .

Taking into account the properties of the dual representation of forces (Section 2.3), the dual region representing the forces that satisfy the contact-point condition is the cone $\widehat{m'n'}$, where m' and n' are the dual lines of the extremes of \overline{MN} , i.e. $\widehat{m'n'}$ contains the dual points of the lines of forces crossing \overline{MN} . The dual region representing the forces that satisfy the direction condition is the cone $\widehat{a'b'}$, where a' and b' are, respectively, lines orthogonal to a and b passing through the origin. Then, as it illustrated in Fig. 12, $\mathbf{G}'_i = \widehat{m'n'} \cap \widehat{a'b'}$.

The generalized force domain \mathbf{G}_S of a contact situation involving a set S of basic contacts is the set of forces resulting from the composition of all the possible compatible reaction forces, one at each basic contact. Let s be any sub-set of S with n non-redundant basic contacts. Then:

$$\mathbf{G}_S \supset \bigcup_{\forall s \subset S} \mathbf{G}_s. \tag{2}$$

Its dual representation, \mathbf{G}'_S , is computed with a recursive algorithm [21] given by:

$$\mathbf{G}'_S = \left[\bigcup_{\forall s \subset S} \mathbf{G}'_s \right] \cup [\mathbf{H}'_S], \tag{3}$$

where \mathbf{H}'_S is a simple geometric region in the dual plane associated to the basic contacts of S : for one basic contact $\mathbf{H}'_S = \mathbf{G}'_s$ is computed as the intersection of two cones as detailed above; for two basic contacts \mathbf{H}'_S is the union of four trapeziums; for three basic contacts it is a triangle, and it is an empty region for more than three basic contacts.

4.3.3. Distinguishability procedure. Force domains are used for contact analysis considering the following points:

- (a) when the generalized force domains of the possible contact situations do not overlap, they enable with certainty the identification of the actual contact situation;

(b) when a configuration is compatible with a contact situation involving a set S of basic contacts, force domains cannot be used to decide with certainty which contacts of S actually take place when contact occurs, since $\mathbf{G}'_s \subset \mathbf{G}'_S \forall s \subset S$.

Let $C(c)$ be the set of $n \geq 1$ contact situations C_{S_1}, \dots, C_{S_n} compatible with a configuration c , such that $S_i \not\subset S_j$ and $S_j \not\subset S_i, \forall i, j \in 1, \dots, n$. Then, if $\mathbf{G}'_{S_i} \cap \mathbf{G}'_{S_j} = \emptyset \forall S_i, S_j \in C(c)$, the configuration is labelled as distinguishable, and as non-distinguishable otherwise.

4.4. Path evaluation algorithm

Figure 13 shows the evaluation algorithms: The algorithm **Path-Evaluation(\mathcal{P})** classifies a path \mathcal{P} depending on the evaluation of a set of its configurations obtained with a uniform sampling of the path; the algorithm **Configuration-Evaluation(c, \mathbf{v})** classifies the path configurations using the following functions that implement the tools presented in the previous section:

Path-Evaluation(\mathcal{P})	Configuration-Evaluation(c, \mathbf{v})
<pre> t = 0 g = 0 P = discretize P FOR ALL c ∈ P r = Configuration-Evaluation(c, v) IF r = AMBIGUOUS THEN RETURN AMBIGUOUS ELSE IF r = GUARDED THEN g = 1 ELSE IF r = COMPLIANT THEN t = 1 END FOR IF g = 1 THEN RETURN GUARDED ELSE IF t = 1 THEN RETURN COMPLIANT RETURN FREE </pre>	<pre> S := Compatibility(c) k := cardinality(S) IF k = 0 THEN RETURN FREE ELSE IF k = 1 THEN n := Motion-Region(c, s₁, v) IF n = 0 THEN RETURN FREE ELSE IF n > 0 RETURN COMPLIANT ELSE RETURN GUARDED ELSE i := 1 m := -4 DO n := Motion-Region(c, s_i, v) IF (m < 0 AND n > 0) THEN m = n i := i + 1 WHILE (i ≤ k AND (n = 0 OR n = m)) IF i = k THEN IF m < 0 THEN RETURN FREE ELSE RETURN COMPLIANT d := Distinguishability(c) IF d = TRUE THEN RETURN GUARDED ELSE RETURN AMBIGUOUS </pre>

Figure 13. Evaluation algorithms.

- $S = \text{Compatibility}(\mathbf{c})$: Given a configuration \mathbf{c} the function returns the set S of basic contacts with which it is compatible.
- $m = \text{Motion-Region}(\mathbf{c}, s_i, \mathbf{v})$: Given a configuration \mathbf{c} compatible with a basic contact $s_i \in S$ and a velocity command \mathbf{v} , the function returns, if possible, the label (1 to 6) of the motion region of s_i containing \mathbf{v} if \mathbf{v} is error-corrective, or -1 if it is not error-corrective. When \mathbf{v} does not belong to any motion region the function either returns 0 if \mathbf{v} produces a break of contact, -2 if it belongs to the friction cone region, or -3 if it cannot be determined due to uncertainty.
- $d = \text{Distinguishability}(\mathbf{c})$: Given a compatible configuration \mathbf{c} the function returns a flag d indicating if it is a distinguishable configuration.

5. EXPERIMENTAL VALIDATION

Experimental validation of the proposed method has been done planning and executing assembly tasks with a Stäubli RX-90 robot equipped with a JR3 force sensor. The robot and the sensor are controlled by an external computer that implements a compliant control [22] by using the real-time path-modification mode of the robot, with a cycle time of 16 ms.

A path planner based on an exact partition of \mathcal{C} -space is used to obtain the nominal plan [23]. The planner partitions $\mathcal{C}_{\text{free}}$ and builds a graph whose nodes are configurations of the border between cells. The arcs of the graph are free paths inside cells that connect any two nodes of each cell. Graph searching techniques, based on the Dijkstra algorithm, are used to find the solution path on the graph.

The experiment described here corresponds to the assembly of an L-shaped part into a T-shaped hole (the largest side of the L-shaped part measures 15 cm). The path planner generates a graph composed of 693 nodes and finds a nominal solution path, composed of 13 arcs, connecting the initial and the goal configurations (Fig. 14a).

The maximum deviations produced by the global and the local sources of uncertainty are $\epsilon_G = 3$ mm and $\epsilon_L = 1$ mm. The nominal solution path is evaluated as guarded, after having evaluated 525 of its configurations in about 20 s on a SGI Octane. As an example, Fig. 14b shows one of the compatible configurations of the path that is evaluated as guarded. At this configuration two contact situations can take place, #1 involving basic contact (V_1, E_1) and #2 involving basic contact (V_2, E_2) , since \mathbf{U}_L^1 intersects $f'_1(\phi_o)$ and \mathbf{U}_L^2 intersects $f'_2(\phi_o)$. The contact situation involving the two contacts cannot occur since when \mathbf{U}_L^1 and \mathbf{U}_L^2 are both centered at the same point of \mathbf{U}_G (the one closest to both $f'_1(\phi_o)$ and $f'_2(\phi_o)$) they intersect neither $f'_1(\phi_o)$ nor $f'_2(\phi_o)$.

The motion analysis tool classifies the commanded velocity at this configuration as non-error-corrective at contact situation #2, and, therefore, classifies the configuration as non-motion-feasible. Finally, the distinguishability analysis tool determines that the configuration is distinguishable because the generalized force

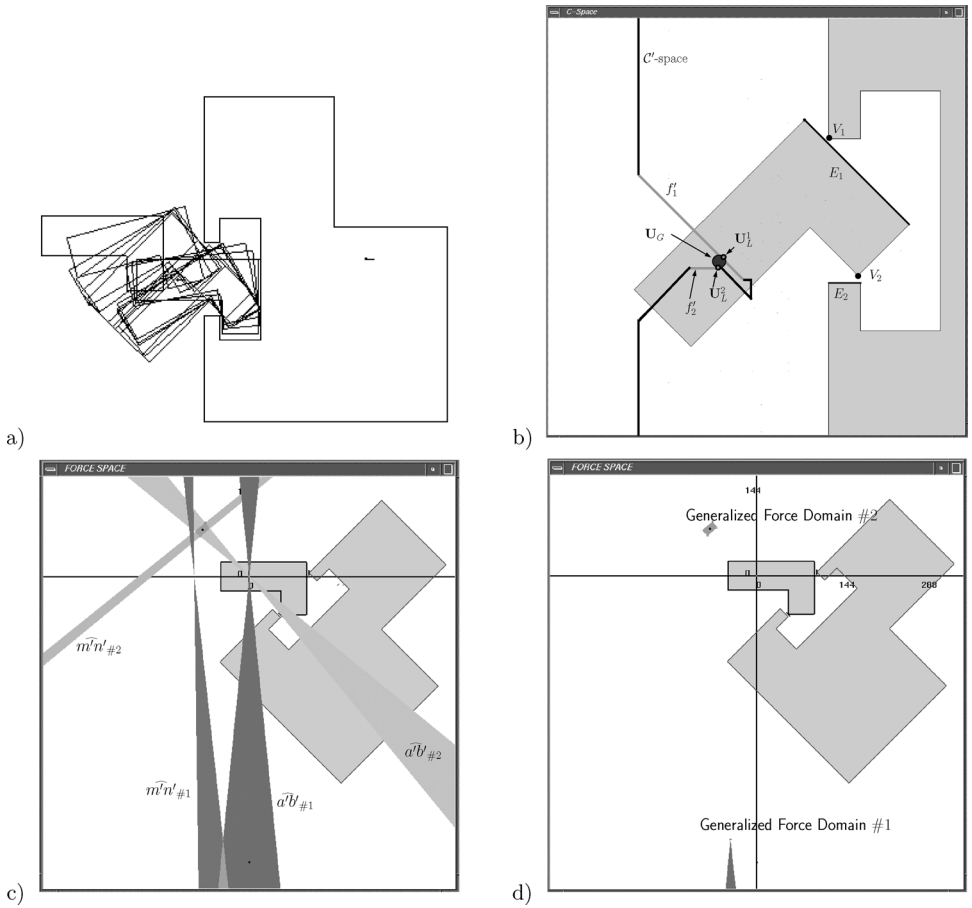


Figure 14. (a) Solution path in C_{free} ; (b) contact position domains used for the compatibility analysis; (c) dual space force analysis and (d) generalized force domains used for the distinguishability analysis.

domains of the two contact situations do not overlap. Figure 14c shows their construction by the intersection of cones $\widehat{m'n'}$ (contact-point condition) and cones $\widehat{a'b'}$ (direction condition), following the procedure detailed in Section 4.3.2 and Fig. 14d the obtained domains used for the distinguishability analysis.

As a result of this analysis the configuration is classified as guarded and a recovery path has been planned from the contact situation #2. When the robot executes the path through this configuration either no contact occurs, or a contact takes place and is identified. If contact #1 occurs the motion proceeds complying at it; otherwise contact #2 takes place and the recovery path is executed. Figure 15 shows some snapshots of the task execution (the second one corresponding to the configuration analyzed here).

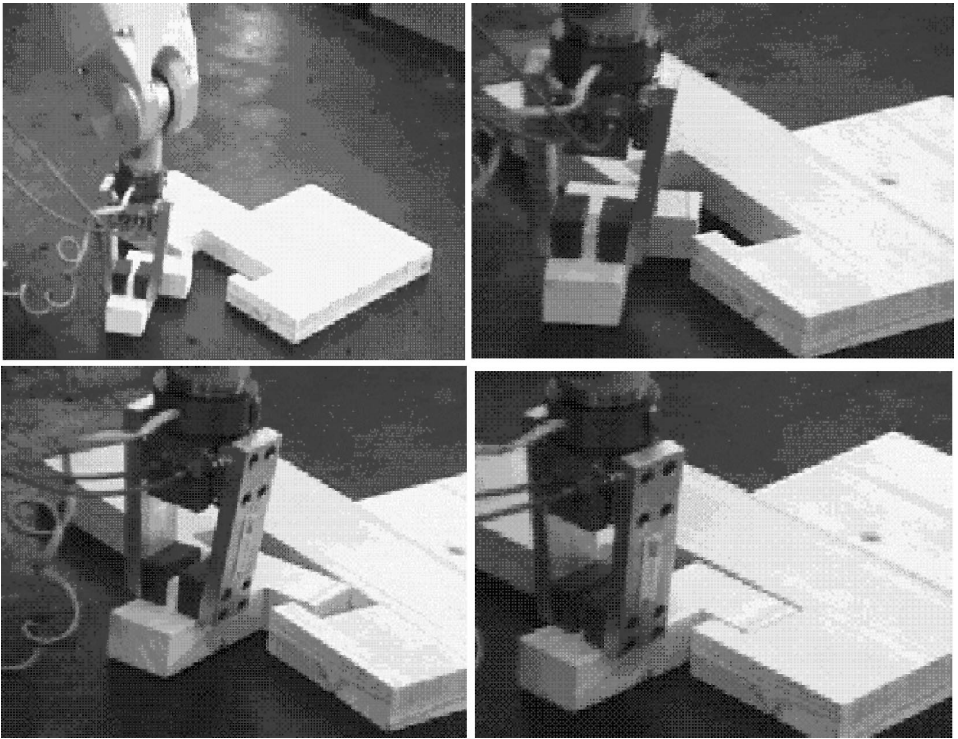


Figure 15. Snapshots of the real task execution of the path.

6. DISCUSSION

Can a given assembly task with uncertainty be executed by a robot if the motions are planned using the nominal geometry? Is this information worthwhile? To answer these questions this paper proposed a method to predict the behavior of motions when contacts are possible due to uncertainty, assuming a compliant robot control. This method, based on three analysis tools and implemented for 3-d.o.f. planar assembly tasks, analyzes the effects of all the uncertainty sources affecting the task and is able to answer whether the nominal path allows to reach the goal despite possible contacts during task execution, i.e. whether the path is feasible or not. This information is worthwhile, because it enables the extension of gross-motion planning techniques to constrained-motion planning problems.

The proposed method analyzes the possible occurrence of contacts at some configurations of the nominal path. This is done using configuration domains that allow to easily handle contact analysis in the presence of uncertainty because they capture the effect of uncertainty and permit to verify the possible occurrence of contacts using the nominal configuration space. For contact situations involving several basic contacts the scope of each source of uncertainty is taken into account, i.e., configuration domains are defined both for the set of local and the set of global sources of uncertainty.

Then, for each possible contact configuration, it is necessary to know if the motion can comply and evolve towards the goal or, if not, whether it is possible to know with certainty which contacts take place. This analysis is done using the motion regions and the generalized force domains defined using the dual representation of forces. The proposed approach has been successfully validated by real experiments.

The extension to assembly tasks in the 3D space can follow the same general procedure, although in this case the complexity of the three analysis tools becomes considerable because they have to cope with the 6-dimensional configuration and force spaces. Based on the experience acquired in the 3-d.o.f. planar case, some simplifications are currently being developed in order to make the approach implementable for the 6-d.o.f. case.

Acknowledgements

The work was partially supported by the CICYT projects DPI2002-03540 and DPI2004-03104.

REFERENCES

1. T. Lozano-Perez, M. T. Mason and R. H. Taylor, Automatic synthesis of fine-motion strategies, *Int. J. Robotics Res.* **3** (1), 3–24 (1984).
2. R. C. Brost and A. D. Christiansen, Probabilistic analysis of manipulation tasks: a conceptual framework, *Int. J. Robotics Res.* **15** (1), 1–23 (1996).
3. S. M. LaValle and S. A. Hutchinson, Evaluating motion strategies under nondeterministic or probabilistic uncertainties in sensing and control, in: *Proc. IEEE Int. Conf. Robotics Automat.*, Minneapolis, MN, pp. 3034–3039 (1996).
4. S. N. Gottschlich and A. C. Kak, AMP-CAD: an assembly motion planning system, in: *Proc. IEEE Int. Conf. Robotics Automat.*, Nice, pp. 2355–2360 (1992).
5. B. J. McCarragher, G. Hovland, P. Sikka, P. Aigner and D. Austin, Hybrid dynamic modeling and control of constrained manipulation systems, *IEEE Robotics Automat. Mag.* **4** (2), 27–44 (1997).
6. J. Xiao and R. Volz, On replanning for assembly tasks using robots in the presence of uncertainties, in: *Proc. IEEE Int. Conf. Robotics Automat.*, Scottsdale, NY, pp. 638–645 (1989).
7. R. Suárez, L. Basañez and J. Rosell, Using configuration and force sensing in assembly task planning and execution, in: *Proc. IEEE Int. Symp. Assembly Task Planning*, Pittsburgh, PA, pp. 273–279 (1995).
8. J. Xiao and X. Ji, On automatic generation of high-level contact state space, *Int. J. Robotics Res.* **20** (8), 584–606 (2001).
9. J. Xiao and L. Zhang, Contact constraint analysis and determination of geometrically valid contact formations from possible contact primitives, *IEEE Trans. Robotics Automat.* **13** (3), 456–466 (1997).
10. J. Xiao, Goal-contact relaxation graphs for contact-based fine motion planning, in: *Proc. IEEE Int. Symp. Assembly Task Planning*, Marina del Rey, CA, pp. 25–30 (1997).
11. H. Asada, Representation and learning of nonlinear compliance using neural nets, *IEEE Trans. Robotics Automat.* **9** (6), 863–867 (1993).
12. V. Gullapalli, J. A. Franklin and H. Benbrahim, Acquiring robot skills via reinforcement learning, *IEEE Trans. Control Syst.* **14** (1), 13–24 (1994).

13. J. M. Schimmels and M. A. Peshkin, Synthesis and validation of non-diagonal accommodation matrices for error-corrective assembly, in: *Proc. IEEE Int. Conf. Robotics Automat.*, Cincinnati, OH, pp. 714–719 (1990).
14. S. Vougioukas and S. Gottschlich, Compliance synthesis for force guided assembly, in: *Proc. IEEE Int. Conf. Robotics Automat.*, Nagoya, pp. 976–981 (1995).
15. T. Lozano-Perez, Spatial planning: a configuration space approach, *IEEE Trans. Comput.* **32** (2), 108–120 (1983).
16. M. Erdmann, On a representation of friction in configuration space, *Int. J. Robotics Res.* **13** (3), 240–271 (1994).
17. J. Rosell, L. Basañez and R. Suárez, Embedding rotations in translational configuration space, in: *Proc. IEEE Int. Conf. Robotics Automat.*, Albuquerque, NM, pp. 2825–2830 (1997).
18. R. C. Brost and M. Mason, Graphical analysis of planar rigid-body dynamics with multiple frictional contacts, in: *Fifth Int. Symp. Robotics Res.*, pp. 293–300 (1989).
19. J. Rosell, R. Suárez and L. Basañez, Path validation in constrained motion with uncertainty, in: *Proc. 14th IEEE/RSJ Int. Conf. Intelligent Robots Syst.*, Maui, HI, pp. 2270–2275 (2001).
20. J. Rosell, L. Basañez and R. Suárez, Contact identification for robotic assembly tasks with uncertainty, in: *Proc. 6th IFAC Symp. Robot Control*, Vienna, Vol. II, pp. 415–420 (2000).
21. L. Basañez, R. Suárez and J. Rosell, Contact situations from observed reaction forces in assembly with uncertainty, in: *Proc. 13th IFAC World Congress*, San Francisco, CA, Vol. A, pp. 331–336 (1996).
22. J. De Schutter and H. Van Brussel, Compliant robot motion II: A control approach based on external control loops, *Int. J. Robotics Res.* **7** (4), 18–33 (1988).
23. J. Rosell, L. Basañez and R. Suárez, Compliant-motion planning and execution for robotic assembly, in: *Proc. IEEE Int. Conf. Robotics Automat.*, Detroit, MI, pp. 2774–2779 (1999).

ABOUT THE AUTHORS



Jan Rosell received the BS degree in Telecommunication Engineering and the PhD degree in Advanced Automation and Robotics from the Technical University of Catalonia, Barcelona, Spain, in 1989 and 1998, respectively. He joined the Institute of Industrial and Control Engineering in 1992 where he has developed research activities in robotics. He has been involved in teaching activities in Automatic Control as Assistant Professor since 1996 and as Associate Professor since 2001. His current technical areas include automatic programming, robotic assembly, motion planning and manufacturing automation.



Luis Basañez received the PhD degree in Electrical Engineering from the Technical University of Catalonia (UPC), Barcelona, Spain, in 1975. From 1976 to 1987 he was Vice-director of the Institute of Cybernetics (UPC) and Director from 1987 to 1990. Since 1986 he is full professor of System Engineering and Automatic Control at the UPC and from 1990, Head of the Robotics Division of the Institute of Industrial and Control Engineering (UPC). He has served as member of the Executive Committee of the International Federation of Robotics (IFR) from 1987 to 1992 and, presently, he is the Spanish Delegate at the IFR. From 1996 he has been a member of the Technical Board of the International Federation of Automatic Control (IFAC). His present research interest includes task planning and coordination of multi-robot systems, sensor integration and active perception.



Raúl Suárez received the Electronic Engineer degree (with honors) from the National University of San Juan, Argentina, and the PhD degree from the Technical University of Catalonia (UPC), Spain, in 1984 and 1993 respectively. He is researcher of the Institute of Industrial and Control Engineering, where he is the Deputy Director, coordinator of the Doctoral Program ‘Advanced Automation and Robotics’ and the responsible for the research line ‘Process Control’. His main research areas include assembly, grasping and manipulation, mechanical hands, task planning and manufacturing automation.